Full Particle-in-Cell Simulation on a Small-Scale Magnetosphere Using Uniform and Nested Grid Systems*)

Toseo MORITAKA[1,2], Masanori NUNAMI[2,3], Hideyuki USUI[1,2] and Tatsuki MATSUI[1,2]

[1]*Kobe University, Nada, Kobe 657-8501, Japan*
[2]*Japan Science and Technology Agency (JST), CREST, Kawaguchi 332-0012, Japan*
[3]*National Institute for Fusion Science, Toki 509-5292, Japan*

(Received 24 December 2010 / Accepted 14 February 2011)

Solar wind interaction with an artificial magnetosphere is investigated by means of a full particle-in-cell simulation. The resultant momentum transfer of solar wind plasmas may provide the propulsive force for a magnetic sail, which is a potential next-generation interplanetary flight system. These simulations are performed using two different simulation codes. One is a traditional code employing a uniform grid system, and the other is a newly developed code with an adaptive mesh refinement (AMR) technique. Even in a small magnetosphere having a scale smaller than the ion inertia length, ions are scattered at the front of the magnetosphere. In this region, an electron-scale current structure is observed, and the electromagnetic interaction with the coil current density, which creates the magnetosphere, causes a propulsive force. The current density structure observed in the AMR simulation is in good agreement with that resulting from the traditional code. The AMR code is expected to be a powerful tool to demonstrate this solar wind interaction under realistic conditions at a reasonable numerical cost.

Keywords: particle-in-cell simulation, adaptive mesh refinement, interplanetary flight system, magnetic sail

DOI: 10.1585/pfr.6.2401101

1. Introduction

Fuel-efficient, robust propulsive systems are essential for deep-space missions. Effective use of the solar wind is a key issue concerning such systems. In a magnetic sail, which was originally proposed by Zubrin [1], the propulsive force is generated by the electromagnetic interaction between the solar wind and an artificial magnetosphere created by a hoop coil inside a spacecraft. Theoretically, the solar wind plasma would be scattered at the front of the magnetosphere, and the resulting momentum loss would be transferred to the spacecraft as a propulsive force.

The spatial scale of the magnetosphere is expected to be quite small, at large on the order of a few hundred meters for a hoop coil having a radius of a few meters. Previous hybrid particle-in-cell (PIC) simulations (fluid electron and kinetic ions) suggest that solar wind ions may be able to pass through such a small magnetosphere without significant interactions because of their inertia effects [2, 3]. Thus far, most simulation studies on magnetic sails have been performed using MHD [4], two-fluid [5], or hybrid PIC [2, 3] codes, and other microscopic effects associated with the electron dynamics and electrostatic interactions in the propulsion mechanism are not yet fully understood.

This article reports the impacts of the electron kinetic effects in the solar wind interaction based on the results of full PIC simulations (kinetic ions and electrons). The spatial scale of the magnetosphere considered in the simulations is less than the ion inertial length. The simulations are performed using uniform and nested grid systems. A newly developed full PIC simulation code [6] with an adaptive mesh refinement technique(AMR) [6, 7] is used for the nested grid simulation. In Sec. 2, the simulation model of the present study is described, and the simulation results are discussed based on the uniform grid simulation. In Sec. 3, the concept of the adaptive mesh refinement code is explained. The validity of the developed code is examined through comparison with the results of the uniform grid simulation. A summary is presented in Sec. 4.

2. Simulation Using a Uniform Grid System

2.1 Simulation model

The present simulations are performed using two-dimensional electromagnetic full PIC code. The time evolutions of the electromagnetic field and super particles are calculated by solving Maxwell equations and the Newton-Lorentz equation, respectively. The simulation domain is given in uniform Cartesian coordinates in the x-y plane, as shown in Fig. 1.

As the initial condition, we consider an uniform plasma flowing in the x-direction. The initial distribution of particles is given by the shifted Maxwell distribu-

author's e-mail: moritaka.toseo@cs.kobe-u.ac.jp
*) This article is based on the presentation at the 20th International Toki Conference (ITC20).

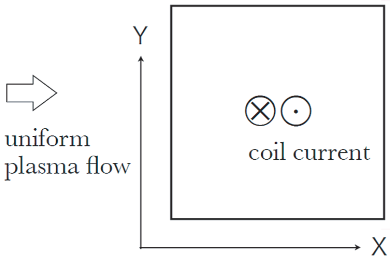

Fig. 1 Schematic diagram of the simulation domain. The anti-parallel current density is supplied at the center of the domain. The solar wind is assumed to be a uniform plasma flow in the $+x$ direction.

tion function with uniform temperature and flow velocity. Anti-parallel current density in the out-of-plane direction is gradually supplied at the center of the simulation domain in the initial phase. This current density corresponds to the modeled coil current and creates a magnetosphere. The fixed boundary condition is applied at the upstream ($-x$) boundary. The super particles are replaced at each time step so as to maintain the distribution function identical to the initial function [8]. In this way, plasmas are supplied continuously from the upstream boundary.

The dimensionless parameters used in the simulation are as follows. The ion-electron mass ratio, temperature ratio, and frequency ratio are set as $m_i/m_e = 25$, $T_i/T_e = 1$, and $\omega_{pe}/\omega_{ce} = 2$, respectively. The initial flow velocity V_{sw} is set to be $V_{sw}/V_a = 2$, where V_a is the Alfven velocity. Here, ω_{ce} and V_a are defined for the unit magnetic field B_0. No background magnetic field is assumed. The spatial profile of the supplied current density is designed so as to create a magnetosphere, the spatial scale L of which is given as $L/S_i \sim 0.4$, where S_i denotes the ion inertial length in the initial uniform plasma. The spatial scale L is defined as the distance between the coil center and the estimated front boundary at which the dynamic pressure of the solar wind balances the magnetic pressure of the magnetosphere.

2.2 Simulation results

Figure 2 (top panel) shows the mass density profile after the set up of the modeled coil current density ($t\omega_{pi} \sim 46.0$). At this time, the interaction process reaches a quasi-steady state, and the Lorentz force acting on the coil current becomes constant. The plasmas injected from the upstream boundary are shielded at the front of the magnetosphere and the low-density region is generated at the downstream side. This indicates that the ions are also scattered with a momentum loss, even if the spatial scale of the magnetosphere is smaller than the ion inertial length. The profile of the out-of-plane current density induced by the plasma flow is shown in Fig. 2 (bottom panel). A thin current structure in the $+z$ direction is found at the front of the magnetosphere. The direction of this current density is opposite to that of the coil current density at the front side,

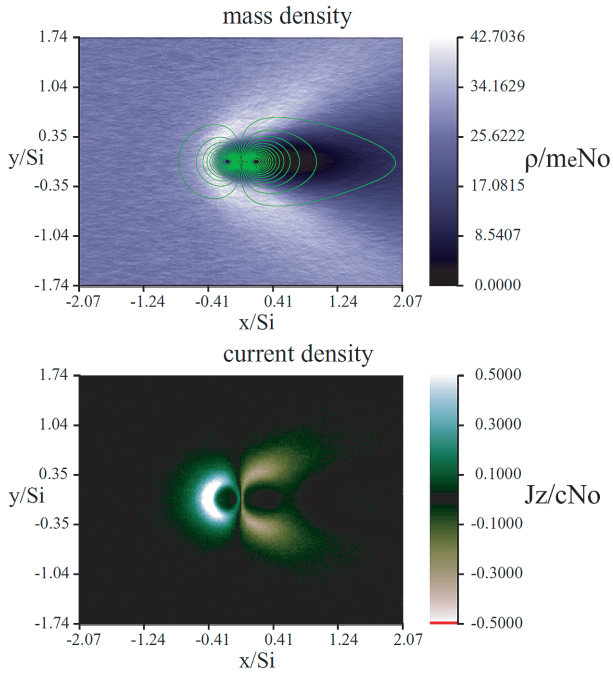

Fig. 2 Color-coded contour plots of mass density and current density at the steady states ($t\omega_{pi} \sim 46.0$). The green lines at the top panel represent magnetic field lines. N_0 denotes the number density of the initial uniform plasma.

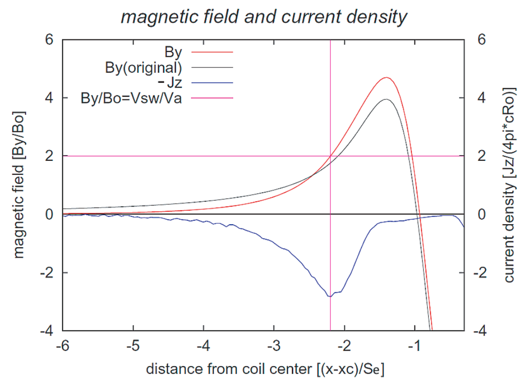

Fig. 3 Profiles of the magnetic field $B_y(x)$ (red line) and current density $-J_z(x)$ (blue line) along the equatorial axis. The black line is the profile of the original magnetic field. The purple lines represent the magnetic field intensity obtained from the pressure balance equation (Eq. 5).

and thus, a repulsive force is generated between the out-of-plane current density and the coil current density. This interaction is the main source of the propulsion force.

Figure 3 shows the profiles of current density $J_z(x)$ (blue line) and magnetic field $B_y(x)$ (red line) along the equatorial line ($y = 0$). The black line represents the original magnetic field generated by the coil current density in a vacuum. The horizontal axis denotes the distance from the coil center normalized by the electron inertial length. In the steady state, the induced current density is related to the deformation of the magnetosphere. The magnetic field in the steady state is given by the sum of the original magnetic field $\boldsymbol{B}^{\mathrm{orig}}$ and the deviation d$\boldsymbol{B}$ from that, i.e., $\boldsymbol{B}^{\mathrm{s}} = \boldsymbol{B}^{\mathrm{orig}} + \mathrm{d}\boldsymbol{B}$. According to Ampere's law, the variation of the magnetic field gradient corresponds to the induced current density:

$$\partial/\partial x(B_y^{\mathrm{orig}} + \mathrm{d}B_y) - \partial/\partial y(B_x^{\mathrm{orig}} + \mathrm{d}B_x) = (4\pi/c)(J_z^{\mathrm{coil}} + \mathrm{d}J_z) \quad (1)$$

$$\rightarrow \partial/\partial x(\mathrm{d}B_y) \sim (4\pi/c)(\mathrm{d}J_z), \quad (2)$$

where $\boldsymbol{J}^{\mathrm{coil}}$ and d$\boldsymbol{J}$ are the coil current density and the induced current density, respectively. Here, we assume that $\partial/\partial t = 0$ for the steady states, $\partial/\partial y = 0$ along the equatorial axis, and

$$\partial/\partial x(B_y^{\mathrm{orig}}) - \partial/\partial y(B_x^{\mathrm{orig}}) = (4\pi/c)(J_z^{\mathrm{coil}}) \quad (3)$$

for the original magnetic field. In the present case, the scale of the magnetic field gradient in the interaction region is comparable to the electron inertia (or gyration) scale.

On the other hand, the strength of the magnetic field at the interaction region is related to the balance between the dynamic pressure of the plasma flow and the magnetic pressure of the magnetosphere. The magnetic field $\boldsymbol{B}^{\mathrm{b}}$ to be balanced with the dynamic pressure is estimated as follows:

$$\frac{1}{2}(\mathrm{m_i} + \mathrm{m_e})nV_{\mathrm{sw}}^2 = \frac{(B^{\mathrm{b}})^2}{8\pi} \rightarrow \frac{B^{\mathrm{b}}}{B_0} = \frac{V_{\mathrm{sw}}}{V_{\mathrm{a}}}. \quad (4)$$

The estimated magnetic field strength B^{b} is indicated by the purple lines in Fig. 3. The observed magnetic field at the interaction region, where the induced current density becomes maximum, corresponds closely to the magnetic field B^{b}. Since the dynamic pressure consists primarily of the ion pressure, this result suggests that the magnetosphere could effectively receive the ion flow, even if its spatial scale is less than the ion inertia length. In this case, the momentum loss of ions might occur through electrostatic interaction with electrons, which are mostly magnetized and pile up at the front of the magnetosphere.

3. Simulations Using an Adaptive Mesh Refinement Technique

The interaction process between the solar wind and the magnetosphere includes a wide range of plasma conditions. For example, the magnetic field strength at the coil surface and the interplanetary magnetic field (IMF) are roughly estimated at O(1 [T]) and O(1 [nT]), respectively. In the case of the kinetic scale magnetosphere, the particle dynamics under the effects of the strong magnetic field near the coil center should be taken into account. The magnetic reconnection between the field lines of the magnetosphere and the IMF is also important. In addition, the plasma density would become quite high near the spacecraft if magnetic inflation [5, 9, 10] by means of plasma injection from the spacecraft is introduced. With traditional codes using uniform size grids, a vast numerical cost is involved in simulating such multi-scale phenomena with different characteristic scales, because the finest grid, capable of resolving the smallest scale, should be used over the entire simulation domain.

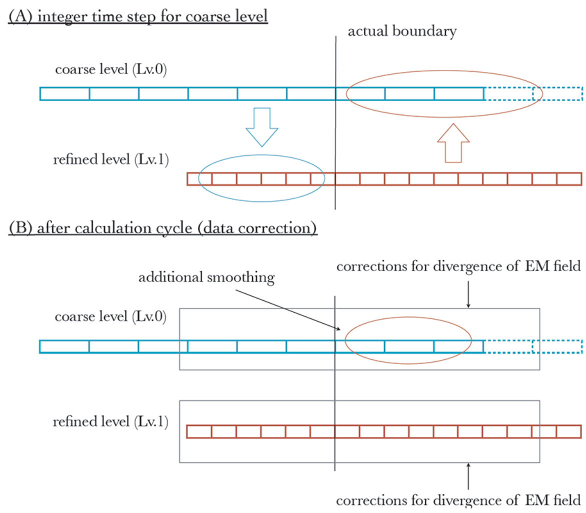

Fig. 4 Schematic diagram of the information exchange at the interface region between two different refinement levels. The top panel (A) show the data exchange process used in the overlap region, and the bottom panel (B) shows the correction processes to the electromagnetic field.

As an approach to quantitative estimation of a magnetic sail using realistic parameters, we have developed a new full PIC code [6] with an AMR technique [7]. In the AMR code, computational grids are refined according to the local conditions and fine grids are allocated selectively to applicable regions. The numerical cost required to simulate multi-scale phenomena can thus be decreased dramatically. The difficulty of the AMR technique lies in the exchange of physical information among different refinement levels with different grid sizes and time step intervals. In order to reduce inconsistencies in the information to be exchanged, we use an overlapping region at the interface [6]. As shown in Fig. 4 (A), physical data is exchanged in the overlapping region at the synchronizing time steps. Additional smoothing and correction of the electromagnetic field in this region is needed in order to relieve aliasing and violation of the conditions with respect to the divergence of the electromagnetic field (Fig. 4 (B)).

Test simulations are performed in order to examine the validity of the AMR PIC code. The simulation conditions used here for the solar wind and the coil current density are identical to those considered in the uniform grid simulation reported in the previous section. Two refinement criteria are used. One is the spatial position of each grid. The grids near the coil center are refined initially, and the arrangement of the refined grids are left unchanged. The other criterion is the magnitude of the local out-of-plane current density and the spatial position. The grids are dynamically refined in regions in which the current density becomes large.

Figure 5 shows the grid arrangement of the hierar-

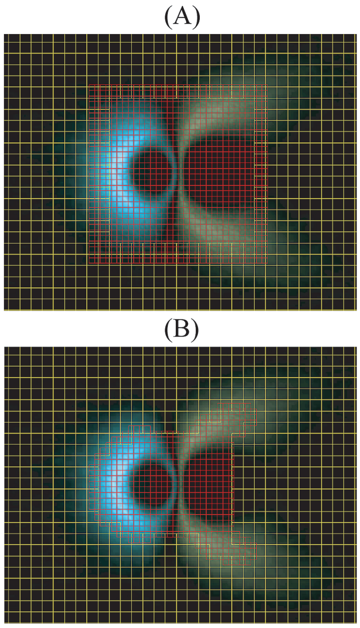

Fig. 5 Arrangement of computational grids used in the AMR simulations. The yellow and red lattices represent the coarse and refined grids, respectively. Each separation corresponds to (4×4) grids. Top (A) and bottom (B) panels show the grid arrangements for the position criterion and for the current density and position criterion, respectively. The color contour represents the current density profile $J_z(x, y)$ for each refinement criterion.

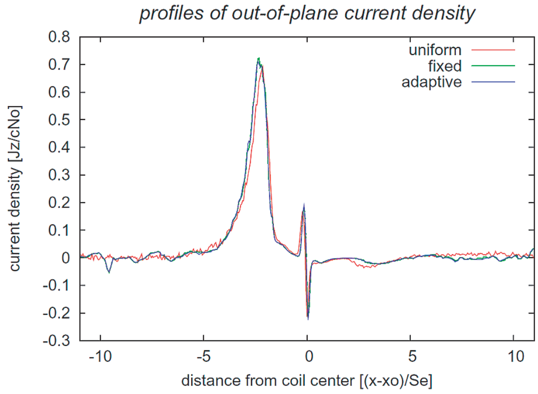

Fig. 6 Profiles of current density $J_z(x)$ along the equatorial line resulting from the uniform grid (red line) and nested grid simulations. The refinement criteria are the spatial position (green line) and the local current density (blue line). The green line overlaps the blue line.

chical grid and the profile of the induced current density resulting from the AMR simulations. The top panel (A) shows the arrangement based on the position criterion, and the bottom panel (B) shows the arrangement for the current density and position criterion. In the bottom panel, the refined grid is produced along the induced current density structure. The current density profile observed in the previous uniform grid simulation (Fig. 2) is duplicated well in the AMR simulations for both refinement criteria. The current density profile along the equatorial line is shown in Fig. 6 (green and blue lines). The observed profiles are quantitatively in good agreement with the profile obtained from the uniform grid simulation (red line in Fig. 6) without any additional distortions due to the presence of the interface between different refinement levels.

4. Summary

Interactions between the solar wind and a kinetic scale magnetosphere, which are relevant to the propulsive mechanism of a magnetic sail, are investigated by full PIC simulation. The spatial scale of the magnetosphere considered in the present study is less than the ion inertial length. An electron-scale thin current structure is observed at the front interaction region of the magnetosphere. The electromagnetic interaction between this induced current density and the coil current is the main source of the propulsion. At this interaction region, ions are also scattered by electrostatic interaction with the piled-up electrons, and the ion dynamic pressure balances the magnetic pressure of the magnetosphere. This result suggests that the momentum transfer to the solar wind would be effective even for a magnetosphere smaller than the ion inertial scale.

In order to realize three-dimensional simulation studies using more realistic parameters, a new full PIC code with an AMR technique has been developed. Validation of the developed code is examined by comparison with a uniform grid simulation for the same simulation conditions. With careful treatment of information exchange at the interface region between different refinement levels, the current density structure at the interaction region resulting from the AMR simulation is observed to be in good agreement with that obtained from the uniform grid simulation.

Acknowledgment

The present study was supported by CREST (JST). Computations were performed using the Plasma Simulator at the National Institute for Fusion Science(NIFS10KTBT018), the JAXA Supercomputer System at the Japan Aerospace Exploration Agency, and the KDK system of RISH at Kyoto University.

[1] R.M. Zubrin and R.G. Andrews, J. Spacecraft and Rockets **28**, 197 (1991).
[2] A. Khazanov *et al.*, J. Propulsion Power **21**, 853 (2005).
[3] Y. Kajimura *et al.*, J. Plasma Phys. **72**, 877 (2006).
[4] H. Nishida *et al.*, J. Spacecraft and Rockets **43**, 667 (2006).
[5] R.M. Winglee *et al.*, J. Geophys. Res. **105**, 67 (2000).
[6] T. Moritaka, M. Nunami and H. Usui, J. Plasma Fusion Res. Series **9**, 586 (2010).
[7] K. Fujimoto, Phys. Plasmas **13**, 072904 (2006).
[8] H. Ohtani and R. Horiuchi, J. Plasma Fusion Res. **4**, 24 (2009).
[9] H. Winske *et al.*, Phys. Plasmas **12**, 072514 (2005).
[10] T. Moritaka *et al.*, IEEE. Trans. Plasma Sci. **38**, 24 (2010).